Integration of grating couplers with a compact photonic crystal demultiplexer on an InP membrane

Tiziana Stomeo, Frederick van Laere, Melanie Ayre, Cyril Cambournac, Henri Benisty, Dries van Thourhout, Roel Baets, T.F. Krauss

Integration of grating couplers with a compact photonic crystal demultiplexer on an InP membrane

Tiziana Stomeo,[1,*] Frederik Van Laere,[2] Melanie Ayre,[3] Cyril Cambournac,[3] Henri Benisty,[3] Dries Van Thourhout,[2] Roel Baets,[2] and Thomas F. Krauss[1]

[1]*School of Physics and Astronomy, University of St. Andrews, Fife KY16 9SS, UK*

[2]*Department of Information Technology (INTEC), Ghent University–Interuniversitary Microelectronics Center (IMEC), B-9000 Ghent, Belgium*

[3]*Laboratoire Charles Fabry de l'Institut d'Optique, CNRS, Campus Polytechnique, Universite Paris-Sud, RD 128, F-91127 Palaiseau, France*

*Corresponding author: tiziana.stomeo@unile.it

We demonstrate the integration of a 30% efficient grating coupler with a compact photonic crystal wavelength demultiplexer (DeMUX). The DeMUX has seven output channels that are spaced 10 nm apart and is aimed at coarse WDM applications. The integrated devices are realized on a high-index-contrast InP membrane using a simple benzocyclobutene wafer bonding technique. Cross talks of −10 to −12 dB for four channels 20 nm apart are obtained without optimization. © 2008 Optical Society of America

OCIS codes: 050.5298, 130.0130, 130.5296.

Compact integration of optical functions on a chip is a key driver to provide low-cost optoelectronic devices that are needed in metropolitan optical networks. High refractive index contrast materials and planar photonic crystal (PhC) technology enable the large-scale integration of optical functions, since waveguides, bends, and core integrated elements can be very compact. Many recent examples of exploiting a large refractive index contrast are provided by silicon-on-insulator (SOI) structures [1–3] and III–V materials in membrane configuration [4]. The SOI platform, is very well suited for performing passive functionality, but it is still rather elusive to achieve active functionality on Si, owing to its indirect bandgap. An emerging solution is to heterogeneously integrate III–V material (active functions) and SOI (passive functions) [5], placing high demands on both. Another solution is to use indium phosphide (InP) compounds, which have been a workhorse for implementing photonic devices with various active functions, such as photodetection, tunability, and carrier injection for gain and lasing. Since such an integration is especially relevant to frequency-selective devices, we use this approach, rather than Si, as the platform for our investigation. Namely, we use a simple benzocyclobutene (BCB) wafer bonding technique [6] to realize InP-membrane-type devices. Using this approach, we present the integration of an efficient grating coupler with a very compact PhC wavelength demultiplexer (De MUX) that operates in the 1500−1560 nm wavelength range.

The one-dimensional (1D) grating coupler (12 μm $\times$ 12 μm) implemented here on top of an Au mirror can achieve a coupling efficiency from standard single-mode fiber to membrane-based waveguides of ~56% [7,8] with relaxed alignment tolerances and relatively large bandwidth. The DeMUX is a membrane version of the device already described in [9–12] for conventional InP heterostructures. It exploits energy transfer caused by intermodal coupling at mini-stop-bands (MSBs) [13,14] of a multimode PhC waveguide. When polychromatic light impinges along the axis of such a waveguide, it essentially feeds the transverse fundamental mode at all frequencies. But, as it experiences propagation along the periodic PhC waveguide, this fundamental mode is coupled to a higher-order mode only for the frequency range within the MSBs. The generated signal, i.e., the WDM signal of interest, is then efficiently and directionally extracted by thinning one of the PhC walls to a few rows. The wavelength selectivity is introduced by varying the central frequency of the MSB, which, in practice, relies on tuning (stepwise or continuously) the PhC waveguide width along the guide.

A typical layout is shown in Fig. 1(a). The PhC waveguide is defined by removing five rows of holes
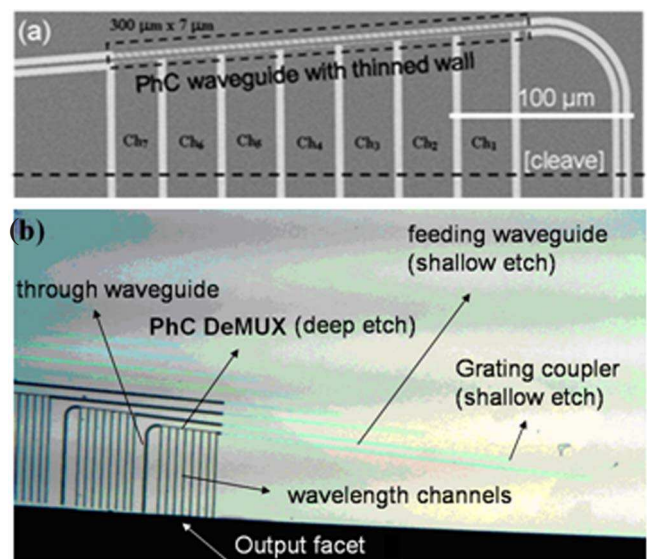

Fig. 1. (Color online) (a) Layout of the PhC DeMUX with seven output channels. (b) Overall test circuit comprising shallow-etched grating and PhC DeMUX, flip chipped and BCB bonded to a host substrate.

("W5") along the ΓK direction, with the PhC cladding on one side thinned down to two rows of holes to extract the higher-order mode. For each channel, a section of ~30 μm in length is sufficient for good extraction, which results in a compact device that successfully compares to, e.g., the approaches of [15–17]. The PhC period is 540 nm, and the filling factor is 41%.

Experimentally, we used a heterostructure consisting (from top to bottom) of a 300 nm InP-membrane layer, a 400 nm InGaAsP etch-stop layer, a 300 nm InP etch-stop layer, and a 400 nm InGaAsP etch-stop layer on an InP substrate. All the etch-stop layers are sacrificial and are removed in the membraning–BCB bonding process. We used a heterostructure with multiple etch-stop layers, although simpler designs are possible. The essential part of the heterostructure is the 300 nm InP guide layer followed by a 400–600 nm (in our case, 522 nm) thick InGaAs etch-stop layer. A noteworthy challenge is that the 1D grating coupler requires shallow etching (~90 nm deep), whereas the wavelength-selective DeMUX has to be deeply etched (~300 nm completely through the membrane layer). To avoid alignment errors, both the coupler and the DeMUX are written in a single step using a Raith Elphy *e*-beam lithography tool. After *e*-beam writing in ZEP520-A positive resist and pattern transfer into the SiO_2 hard mask using reactive ion etching (RIE) with F chemistry, a window is opened by optical lithography to etch the DeMUX first completely through the InP membrane (300 nm). During the first InP etch, the grating coupler and the waveguide are covered with photoresist. The photoresist is then removed, and the whole pattern is etched further to a depth of 90 nm. This means that the DeMUX is etched slightly into the first InGaAsP etch-stop layer. Since this layer will be removed later, however, this is of no consequence. Scanning electron microscope (SEM) pictures of the sample prior to bonding are shown in Fig. 2. A high-quality grating coupler (period of 660 nm and duty cycle of 50%) and PhC DeMUX (hole diameter of 362 nm) with well-controlled sizes were achieved after the pattern is transferred to the InP layer. In the next step, a BCB-buffer layer is spin coated onto the InP die, and Au is deposited opposite the grating couplers. The die is then bonded onto a GaAs host substrate (with another BCB layer), aligning the cleaving planes of both substrates [6].We chose GaAs as the host substrate in the BCB bonding process to facilitate facet cleaving, although other substrates such as SOI or Si are equally suitable. After curing of the BCB, the InP substrate is removed using lapping and wet etching. Finally, all three etch-stop layers are wet etched, the BCB is removed from the holes by inductively coupled plasma (ICP) etching to obtain air holes, and an output facet is cleaved [see optical image in Fig. 1(b)].

To test the integrated device, a single-mode input fiber connected to a tunable laser is positioned at 10° off the vertical axis above the grating to avoid reflections [7]. The 1D grating couples the light into the
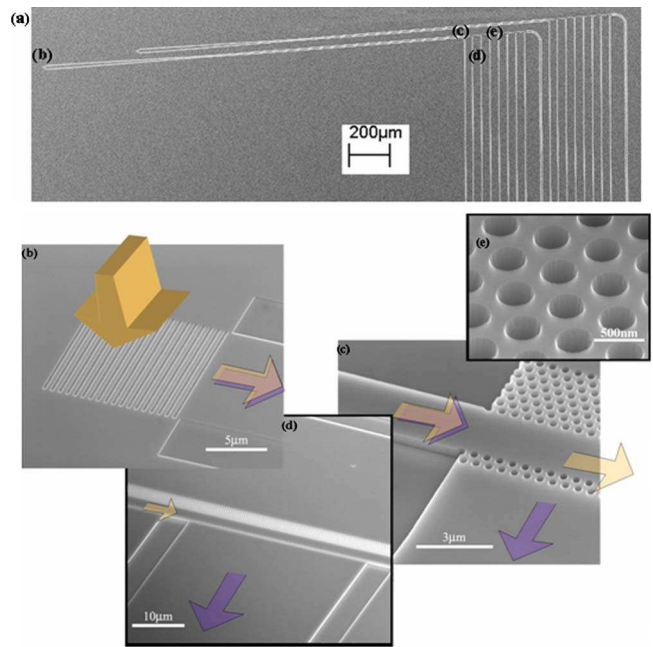

Fig. 2. (Color online) SEM pictures of the devices prior to bonding. (a) Complete device layout: 1D grating coupler integrated with the PhC DeMUX. (b) Input grating coupler (shallow etch). (c) Entrance of the PhC waveguide. (d) Single-channel view. (e) PhC holes (deep etch).

membrane waveguide from where it feeds into the PhC demultiplexer. The optical signal in the seven channels, ranging from 1500 to 1560 nm, is collected at the output facet using a microscope objective lens and measured with a detector. One channel is measured at time while scanning the laser frequency. The demultiplexing operation of the PhC device can clearly be seen in Fig. 3(b). The *Q* factor obtained for the extracted signals as well as the uniform channel spacing of 10 nm are close to those designed. The output signals are normalized to the input grating coupler spectrum determined from a fiber-to-fiber reference measurement on the same sample [see Fig. 3(a)]. The cross talk of the device is −8 to −12 dB for channels spaced by 20 nm. Between adjacent channels (10 nm spacing) it raises up to −4 dB instead of the theoretically predicted value of −7.5 dB. Improvement should result from engineering the transfer function of the MSB, e.g., through fine tuning the size and number of holes of the PhC cladding through which the signal is extracted. Figure 3(c) shows the corresponding coupled-mode modeling [12], which reproduces very well all the spectral details related to the succession of shifted MSBs, for example, the kinks and shoulders of the rightmost channel spectrum. The basis towards further optimization is thus clearly given and hinges on modestly reducing losses and optimizing the section lengths for each channel.

In conclusion, we have demonstrated the integration of two very distinct passive structures on a bonded InP membrane. We combined a shallow-etched 1D grating coupler with a deeply etched PhC DeMUX for operation at the 1500–1560 nm wavelength window. We achieved a good separation of seven optical channels with a spectral resolution of
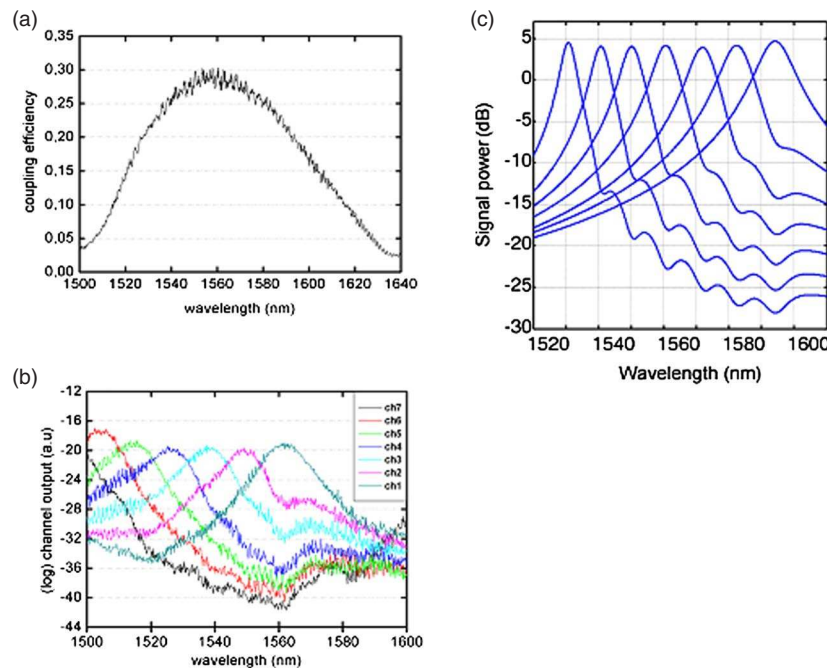
Fig. 3.   (Color online) (a) Grating coupler spectrum control. (b) Channel output normalized to the grating coupler spectrum. (c) Coupled-mode theory modeling rendering most spectral details.

10 nm and −4 dB cross talk, or four channels suitable for coarse WDM (CWDM) at 20 nm spacing with a cross talk of −10 to −12 dB. The typical −10 to −12 dB cross talk for the CWDM 20 nm spacing (every other channel here) can be further improved, all the more because the coupled-mode theory underlying the demultiplexing operation seems fully validated for this first implementation on a membrane. We thus demonstrate a remarkable combination of a nanophotonic strong-index contrast technology and of a design exploiting modes at such a mesoscopic scale that applicability of a revisited coupled-mode approach is granted. This extension of tools that have proven so beneficial to traditional integrated optics in the past and today, in one of the most compact embodiments for demultiplexing [16–18], clearly fosters the perspectives of nanophotonic approaches toward devices of the real world. Along this line, further extension of this work to include detectors and emitters is readily possible, given the InP-based material used in our experiments.

References

1. M. Loncar, T. Doll, J. Vuckovic, and A. Scherer, J. Lightwave Technol. **18**, 1402 (2000).
2. I. Marki, M. Salt, H. P. Herzig, R. Stanley, L. El Melhaoui, P. Lyan, and J. M. Fedeli, Opt. Lett. **31**, 513 (2006).
3. Y. Akahane, T. Asano, B. S. Song, and S. Noda, Opt. Express **13**, 1202 (2005).
4. A. Xing, M. Davanco, D. J. Blumenthal, and E. L. Hu, J. Vac. Sci. Technol. B **22**, 70 (2004).
5. H. T. Hattori, C. Seassal, E. Touraille, P. Rojo-Romeo, X. Letartre, G. Hollinger, P. Viktorovitch, L. Di Cioccio, M. Zussy, L. El Melhaoui, and J. M. Fedeli, IEEE Photon. Technol. Lett. **18**, 223 (2006).
6. G. Roelkens, J. Brouckaert, D. Van Thourhout, R. Baets, R. Notzel, and M. Smit, J. Electrochem. Soc. **153**, G1015 (2006).
7. D. Taillaert, F. Van Laere, M. Ayre, W. Bogaerts, D. VanThourhout, P. Bienstman, and R. Baets, Jpn. J. Appl. Phys. Part 1 **45**, 6071 (2006).
8. F. Van Laere, G. Roelkens, M. Ayre, J. Schrauwen, D. Taillert, D. Van Thourhout, T. F. Krauss, and R. Baets, J. Lightwave Technol. **25**, 151 (2007).
9. E. Viasnoff-Schwoob, C. Weisbuch, H. Benisty, C. Cuisin, E. Derouin, O. Drisse, G. H. Guan, L. Legouezigou, O. Legouezigou, F. Pommereau, S. Golka, H. Heidrich, H. J. Hensel, and K. Janiak, Appl. Phys. Lett. **86**, 101107 (2005).
10. L. Martinelli, H. Benisty, O. Khayam, G. H. Duan, H. Heidrich, and K. Janiak, J. Lightwave Technol. **25**, 2385 (2007).
11. L. Martinelli, H. Benisty, O. Drisse, E. Derouin, F. Pommereau, O. Legouezigou, and G. H. Duan, IEEE Photon. Technol. Lett. **19**, 282 (2007).
12. M. Ayre, C. Cambournac, H. Benisty, O. Khayam, H. Benisty, T. Stomeo, and T. F. Krauss, Photonics Nanostruct. Fundam. Appl. **6**, 19 (2008).
13. S. Olivier, H. Benisty, C. Weisbuch, C. J. Smith, T. F. Krauss, and R. Houdré, Opt. Express **11**, 1490 (2003).
14. S. Olivier, M. Rattier, H. Benisty, C. J. M. Smith, R. M. De La Rue, T. F. Krauss, U. Oesterle, R. Houdré, and C. Weisbuch, Phys. Rev. B **63**, 113311 (2001).
15. T. Niemi, L. H. Frandsen, K. K. Hede, A. Harpoth, P. I. Borel, and M. Kristensen, IEEE Photon. Technol. Lett. **18**, 226 (2006).
16. Y. Akahane, T. Asano, H. Takano, B.-S. Song, Y. Takana, and S. Noda, Opt. Express **13**, 2512 (2005).
17. J. Brouckaert, W. Bogaerts, P. Dumon, D. Van Thourhout, and R. Baets, J. Lightwave Technol. **25**, 1269 (2007).
18. W. Lijun, M. Mazilu, T. Karle, and T. F. Krauss, IEEE J. Quantum Electron. **38**, 915 (2002).